Journal of Materials Chemistry C

Accepted Manuscript

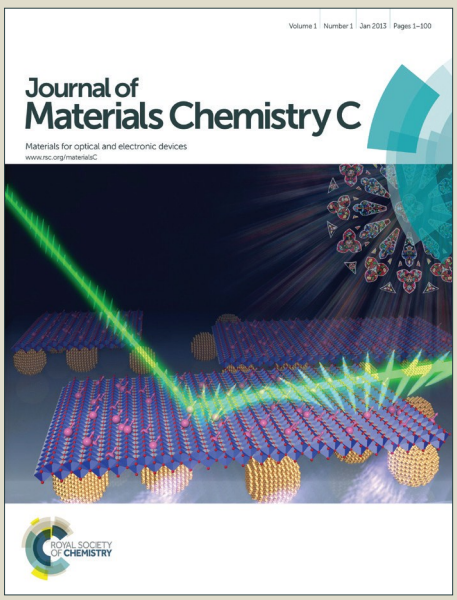

ROYAL SOCIETY OF CHEMISTRY

www.rsc.org/materialsC

Title: The Synthesis of CdTe/ZnS Core/Shell Quantum Dots Using Molecular Single-Source Precursors.

Authors: Shohei Taniguchi and Mark Green

Address: The Department of Physics,

King's College London,

The Strand, London,

WC2R 2LS, UK.

mark.a.green@kcl.ac.uk

Whilst single-source precursors have emerged as an effective method of preparing semiconductor quantum dots, few single-source precursors have been employed for cadmium telluride quantum dots despite the materials exhibiting a wide range of size quantisation effects. In this paper, we explore the use $Cd(TePh)_2$ with amine solvents and capping agents to yield CdTe particles, and also report on the use of a common zinc dithiocarbamate to prepare a ZnS shell, making the synthetic procedure based entirely on single molecular precursors.

Introduction

A myriad of synthetic methodologies have been developed for colloidal quantum dot (QD) synthesis, which enable one to prepare monodispersed, high quality nanomaterials.[1] It is noteworthy that most of the synthetic methodologies for novel compound semiconductor QDs, particularly for II-VI semiconductors, have stemmed from the organometallic thermolysis of molecular precursors in a hot organic solvent; typically described as the "TOPO method", where a chalcogen precursor dispersed in trioctylphosphine (TOP) is reacted with a metal precursor in hot surfactant/solvent (at temperatures up to 350 °C), leading to the formation of the QDs.[2] This method also covers advances that describe the use of other solvents and capping agents using essentially the same methodology. Despite being a sophisticated route, the TOPO method (or any other synthetic method using separate precursors) has limitations because the

nature of nanocrystal formation strongly depends on the reaction of two (or more) constituent precursors (monomers) with differing chemical properties and reactivities. The properties of each precursor (e.g. inherent purity, reactivity and stability) are critical factors, as subtle changes in reaction precursor conditions effect the morphology and optical properties of the nanomaterials; hence, difficulties in reproducibility.[3] Early studies towards mercury and lead containing semiconductor compounds were also limited by the use of dangerous lead and mercury alkyls, which was easily circumvented by the use of single-source precursors (SSPs).[4,5]

An organometallic single-source precursor is a compound having both anion and cation atoms already bound with preformed ionic bonds[6] between, in the case of II-VI materials, the metal and chalcogen. Additionally, the use of SSPs can exclude unfavourable uncertainties arising from the dual-precursors system, where the quick injection of precursors at higher temperature and the subsequent diffusion-controlling nucleation are required.[3,7] The prime application of SSPs is in thin film fabrication using metal organic chemical vapour deposition (MOCVD), where SSPs for a variety of compound semiconductors have been synthesised in order to obtain homogeneous high quality thin films.[8]

Molecular SSPs for colloidal nanomaterials have also been studied from the historically early stages of nanoparticle synthesis. Molecular precursors with the $M(ER)_2$ structure (M = Zn, Cd, Hg, E = S, Se, Te and R = short alkyl or phenyl group) were synthesised in the mid-1980s by Osakada *et al.* and Steigerwald *et al.,*[9,10] where notably Steigerwald reported that $Cd(SePh)_2$ when heated to reflux in 4-ethylpyridine yielded particle-like CdSe clusters with a distinctive excitonic peak in the absorption spectrum.[11] Subsequently, a systematic study using analogous SSPs based on $M(EPh)_2$ was carried out by the same group, showing early evidence of nano-crystalline CdSe, CdTe and HgTe particles,[12] although few optical properties or in-depth studies were reported. Furthermore, the synthesis of colloidal nanomaterials using these precursors appeared to be limited due to their polymeric nature and the difficulty in isolation of the resulting particles. Other SSPs are clearly very effective however; O'Brien and co-workers have pioneered the use of a number of SSPs in colloidal QDs synthesis and the group have reported the synthesis of (amongst others) CdS, CdSe and ZnSe nanocrystals using molecular SSPs of metal dithio/diselenocarbamate and metal imino-bis(diisopropylphosphine selenide) compounds, yielding colloidal II-VI nanocrystals with impressive optical properties suggesting the quantum size effects.[6, 13-18] Other notable related example includes $Zn(TePh)_2$ and organometallic complexes such as $[M_{10}Se_4(SPh)_{16}]^{4-}$ (M = Cd, or Zn).[19,3]

Whilst a number of cadmium chalcogenide nanocrystals such as CdS and CdSe have been prepared using SSPs, little is reported regarding the synthesis of CdTe nanocrystals using such methods. Synthetic challenges in tellurium-containing SSP may hinder further progress in CdTe-based material fabrication, despite an apparent chemical analogy between tellurium, sulfur and selenium. Early reports showed that $Cd(TePh)_2$-1,2-bis(diethylphosphino)ethane (DEPE) complexes dissolved in 4-ethylpyridine, when heated at 168 °C, resulted in nanoparticulate CdTe with an exciton peak at 600 nm.[5] Other CdTe-based SSPs such as $Cd[(TePiPr_2)_2N]_2$ have been used for thin films deposition but not for QD synthesis.[8]

In the work reported here, a CdTe SSP was synthesised whilst referring to the previous literature and applied to current QDs synthesis using established solvent and ligand systems.[5] The prepared CdTe QDs were then overcoated with a ZnS shell in order to obtain photo-stable, bright nanoparticles. To maximise the advantages of using molecular SSPs (e.g. scalability, safety and controllability), it is important that the CdTe SSPs also are prepared in an accessible way. In this work, $Cd(TePh)_2$ was chosen as a single-source precursor for CdTe QDs. The synthetic procedure for $Cd(TePh)_2$ was reported by Steigerwald *et al.*[20] who successfully achieved colloidal particle formation *via* pyrolysis of the precursor in a coordinating solvent, yielding quantum dot-sized CdTe colloids.[12] This previous report described materials with no reported emissive properties, possibly due to the solvent system used; the choice of optimised ligands to passivate a QD surface is a key parameter. Despite this, the precursor is promising and we report here the development of a simple preparation of $Cd(TePh)_2$ and its thermolysis with a suitable ligand system, yielding luminescent particles.

The synthesis of the precursor as reported by Steigerwald involved dimethylcadmium and $PhSeSiMe_3$,[20] and a simpler route was preferred. The use of bis[bis(trimethylsilyl)amido] cadmium, $Cd[N(SiMe_3)_2]_2$, towards the cadmium tellurolato complex, $Cd(TePh)_2$ was achieved from commercially available, simple precursors.[21] We utilised $Cd[N(SiMe_3)_2]_2$, prepared from cadmium iodide (CdI_2) and sodium bis(trimethylsilyl)amide, $NaN(SiMe_3)_2$, warming from -196 °C to room-temperature, yielding a clear yellow liquid containing ($Cd[N(SiMe_3)_2]_2$) and a white residue (NaI).[21] This was filtered and reacted with PhTeH which was prepared *in-situ* from the reaction between diphenyl ditelluride $(PhTe)_2$ and $NaBH_4$ in the presence of cadmium precursor.[22] Each reactant addition proceeded at liquid nitrogen temperature (-196 °C) to prevent undesired reactions, and after adding all the necessary precursors, the temperature was gradually increased to room-temperature with stirring. After 1 hour of the reaction, a yellow precipitate ($Cd(TePh)_2$) was observed in diethyl ether, in good agreement with experimental observations from previous reports.[9,20,21] Potential by-products such as diphenyl ditelluride and

bis(trimethylsilyl)amine were removed *via* washing with warm toluene and diethyl ether. Analysis using solution NMR concurred with the previous report from Steigerwald,[20] and inductively coupled plasma mass spectrometry (ICP-MS) of the purified SSPs gave an elemental ratio of Cd:Te = 1.2:2.0, which indicated the formation of $Cd(TePh)_2$. The resulting $Cd(TePh)_2$ was readily dissolved in coordinating solvents such as N,N-dimethylformamide (DMF), pyridine and dimethyl sulfoxide (DMSO). Re-crystallisation of $Cd(TePh)_2$ in DMF yielded yellow needle-like crystals, which were then characterised using ^1H NMR (detailed descriptions are outlined in the experimental section).

Experimental

Cadmium iodide (CdI_2, 99.0 %), sodium bis(trimethylsilyl)amide solution ($NaN(SiMe_3)_2$, 1.0 M in tetrahydrofuran), diphenyl ditelluride (PhTeTePh, 98 %), sodium borohydride ($NaBH_4$, 99 %), zinc diethyldithiocarbamate ($ZnDDTC_2$, 97 %), oleic acid (90 %), anhydrous N,N-dimethylformamide (DMF, 99.8%), dimethyl sulfoxide-d_6 (DMSO-d_6, 99.96 atom % D) were obtained from Sigma Aldrich. Technical grade oleylamine (OAm, 70 %) was obtained from Fluka. All the chemicals were used as received.

TEM was carried out using a Tecnai 20 (acceleration voltage 200 kV) for normal resolution images. Samples were dropped on a copper grid with a carbon amorphous film (Agar Scientific) and dried in ambient conditions. High resolution images were obtained using a JEOL JEM-4000EX HREM at 400 kV. This work was carried out at the Department of Materials, University of Oxford with the support of Dr Teck Lim (C. Hetherington group). Absorption spectroscopy measurements were taken using a Hitachi U-4100 UV-Visible-NIR spectrophotometer in a 1 cm path length quartz cuvette. Emission spectra were obtained using a Perkin Elmer LS 50B spectrometer.

Photoluminescence quantum yields (PL QY) were calculated by comparison with fluorescent standards. Rhodamine 6G (99 %, Sigma Aldrich) was used for the samples excited at 450-500 nm, whilst Rhodamine 101 inner salt (Sigma Aldrich) was used for the excitation at 550 nm. The PL QYs of these standards were obtained from previous reports. [23,24] In a typical procedure, the fluorescence standard was diluted until the absorbance at the excitation wavelength was below 0.1 in order to avoid potential scattering and inner filtering effects. The emission spectrum was then taken with the same solution, and the integrated emission intensity was calculated using the obtained emission spectrum. Then, a plot was produced using the obtained absorbance and the integrated emission intensity. Measuring the absorption and emission spectra were repeated at least four times with the fluorescence standard solution diluted at an

arbitrary ratio from the original solution. The same procedure was followed using the samples using the same measurement settings. The obtained values were then plotted to obtain the integrated emission intensity – absorbance relationship, followed by the calculation of the PL QY.

Solid samples for X-ray diffraction (XRD) were prepared by precipitating QDs with non-solvents several times to ensure no extra surfactant remained. The precipitate was subsequently dried by vacuum pump and stored under nitrogen before use. XRD measurements were taken using a Panalytical X'Pert Pro MPD diffractometer using nickel-filtered copper Kα radiation operating at a voltage of 40 kV and a beam current of 30 mA. Diffraction data were collected using an X'Celerator multiple strip detector. The diffractometer was configured to operate in programmable divergence slit mode with an observed length of 10.0 mm. The specimens were placed onto the surface of a zero-background silicon crystal sample holder during the diffraction experiments. The experimental data were processed using Panalytical Highscore Plus. The program interpolated the data to rationalise the step size to multiples of 0.001°. The data were then transposed to represent a fixed divergence slit configuration with a slit size of 1.00° as this allowed comparison to existing crystallographic databases.

This analysis was performed in ITRI labs, United Kingdom.

$Cd(TePh)_2$ Synthesis

This method was inspired by the reports of the synthesis of $M(TeAr)_2$ (M = Zn, Cd, Hg; Ar = C_6H_5, 4-MeC_6H_4, 2,4,6-$Me_3C_6H_2$).[9,20,21] In a typical reaction, 0.436 g of CdI_2 (1.2 mmol) was put into a 100 mL two-neck flask and flushed by nitrogen three times, then the flask was cooled with liquid nitrogen. To the cooled flask, 2.4 mL of 1 M $NaN(SiMe_3)_2$ solution (2.4 mmol) was slowly injected and allowed to freeze. The reaction flask was taken from the liquid nitrogen and the mixture was gradually warmed to room-temperature with moderate stirring. After 1.5 hours, the mixture separated into yellow liquid ($Cd[N(SiMe_3)_2]_2$) with a white precipitate (NaI), which were separated by filtration and centrifugation under nitrogen.

In a separate 100 mL two-neck flask, 480 mg of $(PhTe)_2$ (2.4 mmol) was dissolved in 10 mL anhydrous diethyl ether under nitrogen, and allowed to stir for 1 hour. Afterwards, the solution was frozen with liquid nitrogen and 50 mg $NaBH_4$ (2.4 mmol) was added.

The yellow Cd-containing solution was taken and injected into the frozen $(TePh)_2$/diethyl ether mixture. The mixture was gradually warmed to room-temperature and stirred for 1 hour, yielding a yellow solid ($Cd(TePh)_2$) which precipitated out of the orange solution.

Purification of $Cd(TePh)_2$

The flask containing $Cd(TePh)_2$ in diethyl ether was sonicated to ensure no solid was attached to the flask wall. Then, all the reactants including the yellow solid were transferred to a centrifuge tube filled with nitrogen. The reagents were then centrifuged at 3,000 rpm for 2 minutes, separating the liquid/solid layers. The supernatant was then discarded and 2 mL anhydrous diethyl ether was added to wash the solid. This wash/centrifuge process was repeated twice using 2 mL anhydrous diethyl ether and 2 mL anhydrous toluene. The resulting yellow $Cd(TePh)_2$ solid in the tube was dried under vacuum to give a fine yellow powder. The resulting $Cd(TePh)_2$ (50 mg) could be readily dissolved by 2 mL anhydrous DMF, yielding a clear yellow solution with a small amount of white insoluble material. Storage at 4 °C or evaporation by vacuum gave yellow crystals. ^{1}H NMR (DMSO-d_6): δ 6.76 (t, 2H), δ 6.96 (t, 1H), δ 7.73 (d, 2H).

CdTe QDs Synthesis from $Cd(TePh)_2$

100 mg of $Cd(TePh)_2$ powder was charged to a centrifuge tube and filled with nitrogen. To the tube, 5 mL of TOP was injected and sonicated for 1 hour, causing a cloudy beige solution. The solution was then centrifuged at 4,000 rpm for 10 minutes, yielding a clear solution (TOP-$Cd(TePh)_2$) with a white precipitate on the bottom. 5 mL of the TOP-$Cd(TePh)_2$ was injected in 10 mL of degassed oleylamine (OAm) at room-temperature. The solution was quickly heated to 200 °C and the solution colour change monitored by absorption spectroscopy. At the point of desired particle size, the reaction was quenched by cooling the reaction medium. The resulting QDs were precipitated by an addition of methanol.

CdTe/ZnS Synthesis

The basic synthetic procedure was taken from Chen *et al.* with some minor amendments.[25] A ZnS SSPs stock solution was prepared by dissolving 360 mg of zinc diethyldithiocarbamate ($ZnDDTC_2$, 1 mmol) in 5 mL TOP, followed by sonicating for 10 minutes. In another flask, 6 mL of purified CdTe QDs (50 μM in hexane) and 10 mL OAm were mixed and the hexane was evaporated at 100 °C for 30 minutes. Then, 0.25 mL of ZnS stock (0.05 mmol) was injected in the CdTe solution at 70 °C. The reaction temperature was then increased to 180 °C for 30 minutes, causing a change in solution colour to brown. Afterwards, the solution was cooled down to 100 °C for the next shell addition. After depositing the desired thickness of the ZnS shells, the crude CdTe/ZnS solution was cooled down to 70 °C and diluted with 3 mL of hexane. The QDs were then precipitated by adding acetone (half volume of the original solution was required to precipitate the QDs). After centrifugation, the solid layer was re-

dispersed in toluene, causing a brown cloudy solution. The remaining insoluble materials could be removed by repeating the purification process.

Discussion

CdTe QDs were synthesised using $Cd(TePh)_2$ as a precursor. As a growing number of synthetic procedures towards QDs have been reported in the last decade, an extensive choice of solvents and surfactant molecules are now available to obtain the desirable characteristics of QDs. In this study, TOP was first used to coordinate and stabilise the CdTe SSP, as phosphines are often thought to be efficient ligands for organometallic compounds. Typically, an excess of TOP (>50 times more than $Cd(TePh)_2$ by molar ratio) was mixed with the CdTe SSP under an inert atmosphere and sonicated in an ultrasound bath until the yellow colour from $Cd(TePh)_2$ faded, giving a clear solution. A similar phenomenon was reported by Jun *et al*., in which pale-yellow coloured $Zn(TePh)_2$ turned to colourless after formation of a $Zn(TePh)_2$-tetramethylethylenediamine complex.[19] After removal of insoluble precipitates by centrifugation, a transparent colourless solution of $Cd(TePh)_2$-TOP was obtained. The prepared $Cd(TePh)_2$-TOP was then injected into degassed oleylamine (OAm) at room-temperature. The solution was then gradually increased (*ca.* 10 °C/min) up to 210 °C, and the solution displayed a light-yellow colouration at 120 °C, followed by the emergence of a red colouration. The observed colour change suggested the formation of nuclei of CdTe QDs, and the absorption spectra are shown in figure 1, showing a gradual red-shift in the absorption profiles. Quantum size effects can be seen from the spectra where the absorption onset was shifted from 530 nm to 680 nm as the band gap energy becomes smaller as the particle size increases. Additionally, the half width at half maximum (HWHM) of the excitonic peaks, which were determined from the centre of absorption peak to the half value of the absorbance in lower energy, were investigated, showing that the HWHM of the absorption profile of CdTe QDs after 10 minutes of the reaction was 18 nm, whilst that of the sample after 55 minutes of heating was 35 nm. (HWHM was used instead of the full width at half maximum (FWHM) as absorption peaks in Figure 1 were asymmetric and the FWHM could not be obtained from the given spectra.) The single observable excitonic peak present throughout the reaction and wide excitonic HWHM in larger particles can be comparable to thiol-stabilised CdTe QDs synthesised in aqueous solution, where the Ostwald ripening process is the major driving force in particle growth.[26,27] It is reasonable that QDs formation using the SSPs has a similar growth dynamics to thiol-stabilised aqueous routes as Cd-Te clusters are thought to be formed already (or instantly) in the solution at lower temperature, where thermodynamics then dominate the particle growth, in contrast to

diffusion-controlling growth dynamics achieved by slow decomposition of metal precursor such as TDPA-Cd in hot solvent.[28,29]

The resulting CdTe QDs showed a tuneable emission wavelength dependant on the particle size (Figure 2a). It is possible to control the emission wavelength continuously from 528 nm to 664 nm. Figure 2 (b) and (c) show the temporal evolution of photoluminescence quantum yield (PL QY) and FWHM of emission profiles at each reaction stage. The PL QY of CdTe QDs prepared through the SSPs route changed depending on peak wavelength, and the maximum PL QY (18 %) was recorded in the sample with an emission peak at 641 nm. The obtained PL QY was not as high as other CdTe QDs, with PL QY typically up to 70%.[26,29,30] The FWHM of the emission profile was in good agreement with the CdTe QDs prepared *via* the aqueous routes, where the values started from as low as 35 nm and increased above 50 nm as the particles grew,[26,27] whilst CdTe QDs prepared by the organometallic route gave smaller FWHM below 30 nm.[29] Despite this, it was possible to improve the quality of the CdTe QDs through the SSPs route by the optimisation of reaction condition and post-synthetic treatment, such as size selective precipitation. Figure 3 shows pictures of purified CdTe QDs in toluene under ambient condition and excitation at 365 nm, confirming their notable fluorescence. Given the optical characteristics, $Cd(TePh)_2$ could be successfully used as an alternative to the conventional dual precursors system for the synthesis of colloidal CdTe QDs. The elemental ratio of the resulting CdTe QDs was investigated using ICP-MS, showing Cd:Te = 1.00:0.74. The cadmium content exceeded the tellurium content in contrast to the elemental ratio in $Cd(TePh)_2$. The result was in good agreement with other reports, where elemental analysis by energy-dispersive X-ray spectroscopy (EDX) gave Cd:Te = 1.0:0.7-0.8.[31,32] Furthermore, the resulting cadmium concentration calculated from ICP-MS showed close values to theoretical value given by the mass of $Cd(TePh)_2$ used in the reaction. The fact indicates that most of the $Cd(TePh)_2$ in solution was successfully consumed to form CdTe QDs with a preferable reaction yield. For example, 100 mg of $Cd(TePh)_2$ (0.19 mmol) resulted in 3.3 nm CdTe QDs solution containing 0.14 mmol of cadmium (73.7 % reaction yield), from the calculation explained in the supporting information.[33] In contrast, the organometallic dual-precursor procedure described elsewhere[34] gave a limited reaction yield; 0.2 mmol of CdO produced 3.9 nm CdTe QDs solution containing only 0.034 mmol of cadmium contents (17% reaction yield).

As interest in the application of colloidal QDs favours biological imaging, it is important to suppress unfavourable effects arising from the nature of cadmium-related materials. Therefore, a ZnS shell deposited on a core surface - one of the best known synthetic treatments of colloidal QDs systems – was investigated. To further simplify the reaction procedure, a SSP

was used as a ZnS source. In this study, zinc diethyldithiocarbamate ($ZnDDTC_2$), a standard shelling precursor used extensively as a precursor for thin film and nanoparticle shell deposition due to its stability.[35] The use of dithiocarbamates as a shelling material has become wide-spread and numerous systems have been reported, such as CdSe/ZnS, CdTe/CdSe/ZnS and CdS/ZnS QDs, all of which displayed enhanced/photo-stable fluorescent characteristics.[25,35,36,] The rationale for the use of $ZnDDTC_2$ in this work is; (i) air stability and ease of handling, (ii) viability of shell deposition as proven by several researchers, and (iii) commercial availability and cost.

In a typical synthesis of CdTe/ZnS QDs, CdTe QDs (emission peak at 610 nm, absorption exciton peak at 557 nm) were precipitated by methanol and re-dispersed in hexane, and then mixed with degassed oleylamine (OAm). To the QDs solution at 90 °C, the $ZnDDTC_2$ (dissolved in TOP) was added and the temperature was increased to deposit the ZnS shell. The amount of ZnS SSPs added was calculated so that only one layer of ZnS should deposit on the CdTe surface (supporting information). The original clear red colour turned slightly cloudy due to the addition of the less soluble $ZnDDTC_2$, then a distinct brown colouration was observed upon heating at 130 °C presumably due to the thermal decomposition of $ZnDDTC_2$ with amines. The solution was stirred at 180 °C for 20 minutes and cooled to 100 °C. The solution was then ready for a second addition of $ZnDDTC_2$ and the same process was repeated six times to ensure sufficient ZnS was formed. The procedure, described as thermal-cycling using single-source precursor, was inspired by the work of Chen *et al.* who reported the deposition of a ZnS shell on CdS using $ZnDDTC_2$.[25]

The absorption spectra of the resulting CdTe/ZnS QDs solution after purification can be seen in figure 4 shows. Although the excitonic peak at 570 nm became less pronounced after each shell addition, there was no significant spectral red-shift observed, which is thought to be a common phenomenon in CdTe/ZnS synthesis.[34,37]

The emission spectra of the resulting CdTe/ZnS QDs were also studied (Figure 5 (a)). No significant shift in the emission wavelength was observed beyond a slight leakage of the exciton into the shell, as was expected when referring to the absorption spectra. Figure 5 (b) shows the change in fluorescence intensity at each ZnS shell deposition stage, indicating a rapid decrease in fluorescence intensity after the first ZnS addition.

Figure 6 shows the emission spectrum of CdTe/ZnS (6th shell addition) excited at shorter wavelength (350 nm). The spectrum showed the emission peak at higher energy (*ca*. 420 nm), which we suggest indicated the presence of other chemical species in the solution (e.g. ZnS nanoparticles), affecting the fluorescence quality of CdTe/ZnS QDs. Whilst it is necessary to investigate the underlying surface chemistry to obtain improved optical properties, it is also important to consider that the correct shell precursor needs to be chosen and that subtle difference in reaction conditions can result in insufficient shell deposition or a drop in emission.[34,36] For example, Smith *et al.* reported emission quenching of CdTe QDs after an addition of Zn and S precursors equivalent to 1 monolayer (ML), whilst 0.5 ML shell addition achieved improved emission.[34] Also, Zhang *et al*. observed successful shell deposition using $ZnDDTC_2$ but failed to deposit a ZnS shell using a dual precursors system with zinc carboxylate and elemental sulfur.[36] One also needs to examine why we observe a drop in emission intensity after shell deposition. The use of a shell layer, whilst generally favourable in the prototypical CdSe/ZnS system, is actually more complex than simply providing a wider band gap barrier. Most core/shells systems based on CdSe/ZnS have a bright point,[38] beyond which the emission drops off and this is well known from the earliest reports of core/shell particles, so a reduction in emission intensity is not unexpected, although this is usually preceded by an increase in quantum yield.

The increase in quantum yield once a shell has been deposited is not always observed. HgTe/CdS core/shell particles reportedly exhibit no improvement in emissive properties over the bare HgTe particles once a shell was grown.[39] Two significant reports detailed the deposition of a CdS or ZnS shells on particles of PbSe/CdSe resulted in significant quenching, attributed to annealing at the core/shell interface.[40, 41]

If we explore the CdTe system, we observe evidence to suggest that simply capping CdTe with ZnS is not simple. One of the earliest reports of CdTe/ZnS made by the organometallic route using traditional precursors described only a slightly higher quantum yield than the bare sample, although not details were given.[42] In related work, samples of CdTe/CdS prepared by organometallic precursors have shown an initial high quantum yield which was observed to rapidly drop to almost zero upon prolonged shell growth and heating.[43] The growth technique here also plays a role – where the addition of simple precursors does not appear to give a robust shell, the SILAR route does appear to give better samples.[34] We should also appreciate that we have a single source precursor, which is only ca. 22 % atom efficient resulting in the introduction of decomposition product organic groups into the growth solution with Lewis Base

functionalities, which will have a distinct impact on the QD produced.[44] We therefore suggest that further work is required to optimise the ideal shell material and growth condition for CdTe.

Electron microscope images of CdTe QDs (before and after ZnS addition) are shown in Figure 7 (a, b). The CdTe QDs appeared to be spherical, although aggregated making it difficult to identify individual nanoparticles. The observed aggregation could be explained by the lower coordinating capability of primary amines as ligands.[45, 46] Particularly, it has been reported that two to three purification steps by precipitation with non-solvents caused almost complete removal of hexadecylamine from the surface of CdSe QDs.[47] It is therefore reasonable to assume that the same effect occurred on our nanoparticles given the similarity in the system. The electron micrograph of CdTe/ZnS QDs can be seen in Figure 7 (b). Although individual particles could be observed, rod-like materials were also observed, adjacent to the spherical particles. Figure 7 (c) shows the size distribution of obtained CdTe and CdTe/ZnS QDs calculated by measuring approximately 150 particles for each sample. The average diameter of each sample was 3.1 ± 0.9 nm for CdTe and 3.7 ± 0.7 nm for CdTe/ZnS QDs. Given the amount of ZnS precursor added (4ML equivalent) and estimated thickness of a ZnS monolayer (0.31 nm), theoretical prediction of the diameter of CdTe/ZnS QDs would be *ca.* 5.6 nm. There is a substantial difference between obtained and estimated diameter on CdTe/ZnS QDs and this is possibly due to an insufficient deposition of ZnS on the CdTe surface and unwanted nucleation of ZnS clusters, or the anisotropic growth giving non-spherical rod-like structures. The growth of rod-like structures during shell deposition has been previously observed with CdSe/CdS, where usually simple spherical particles were expected.[48]

The crystal phase of the resulting QDs was studied using X-ray diffraction (XRD) analysis. Figure 8 shows the XRD patterns of CdTe QDs and CdTe/ZnS QDs prepared from SSPs. The patterns showed the domination of the shell structure of the QDs after shell deposition; whilst CdTe QDs indicates a zinc blende (cubic) structure, CdTe/ZnS QDs clearly shows the characteristics of wurtzite (hexagonal) ZnS. Notably, the peak at 24° (2θ) of the original CdTe QDs shifted after the shell formation, we can therefore conclude that the internal crystal structure of the CdTe core was affected by the ZnS shell, rather than maintaining the structure. It is somewhat unusual, as other reports using $ZnDDTC_2$ showed that XRD patterns after ZnS deposition were predominantly zinc blende structure;[36, 25] the formation of wurtzite ZnS is less common compared to zinc blende ZnS. There are a limited number of papers showing the XRD patterns of wurtzite ZnS nanocrystals, where, for example, diethyl zinc/bis(trimethylsilyl)sulfide, or zinc ethylxanthate were decomposed in organic solvents.[49, 50, 51] We suggest that the crystal structure of a ZnS shell does not only depend on the type of

precursors; other factor such as core crystals, reaction solvent, temperature and surfactants also affect the final crystal structure. It is also possible that the XRD pattern is from separate ZnS nanoparticles not on the CdTe core (i.e. individual particles). However, we would expect the pattern from the core particles to still be visible, which is not the case.

We also explored changes in reaction condition and the outcomes for the synthesis of CdTe QDs. Reaction conditions were the same as those described in the experimental section unless otherwise noted. As discussed in many previous studies, solvents and capping agents are major factors for directing particle growth. Whilst long chain alkylamines such as hexadecylamine (HDA) had virtually the same effect as oleylamine (OAm), carboxylic acids and phosphonic acids caused immediate precipitation with the absence of any emission from the precipitate. The influence of reaction parameters on the synthesis of the shell was also explored. The use of either Et_2Zn or $Zn(NO_3)_2$ with sulfur dissolved in trioctylphosphine at deposition temperature between 180 ºC and 210 ºC resulted in similar reductions in emission intensity after 3 shells had been deposited, accompanied with a red shift in the emission profile, consistent with previous reports. [34,37] The use of octadecene as a solvent for the shell single source precursor also resulted in a significant decrease in emission intensity.

Conclusion

Colloidal CdTe QDs were synthesised in oleylamine using $Cd(TePh)_2$ coordinated with TOP. The resulting QDs showed quantum size effects and their particle size could be controlled by changing reaction times to produce QDs emitting from the green to the red region of the visible spectrum with a maximum quantum yield of 18% (emission peak of 647 nm). The single source precursor $ZnDDTC_2$, was used to deposit a ZnS shell on the CdTe core, resulting in an overall fluorescence intensity decrease as the ZnS shell formed. TEM results showed spherical particles of both CdTe and CdTe/ZnS QDs having diameter of 3.1 ± 0.9 nm and 3.7 ± 0.7 nm, respectively. An XRD study suggested that the hexagonal phase dominated after ZnS shell deposition on the CdTe core. The synthesised $Cd(TePh)_2$ showed excellent potential as one of the few single source precursors available for CdTe QDs synthesis, whilst the optimisation of optical characteristics and the stability of CdTe/ZnS QDs are currently underway.

Acknowledgments

We acknowledge Andy Cakebread (King's College London) for mass spectrometry and ITRI (St. Albans, UK) for XRD analysis. We also acknowledge the Centre for Ultrastructural Imaging, King's College London for electron microscopy. We also acknowledge the Japan Student

Services Organization (JASSO), the British Council Japan Association (BCJA) and King's College London (King's Overseas Research Studentship) for funding (ST).

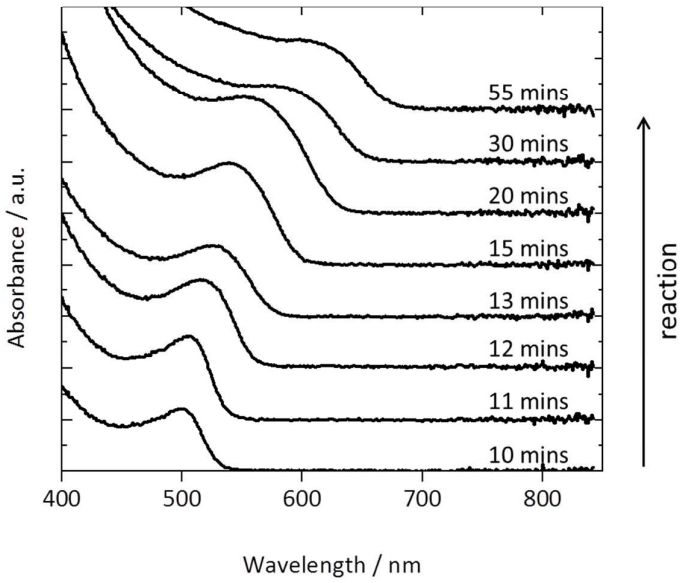

Figure 1. Absorption spectra observed during CdTe quantum dot growth.

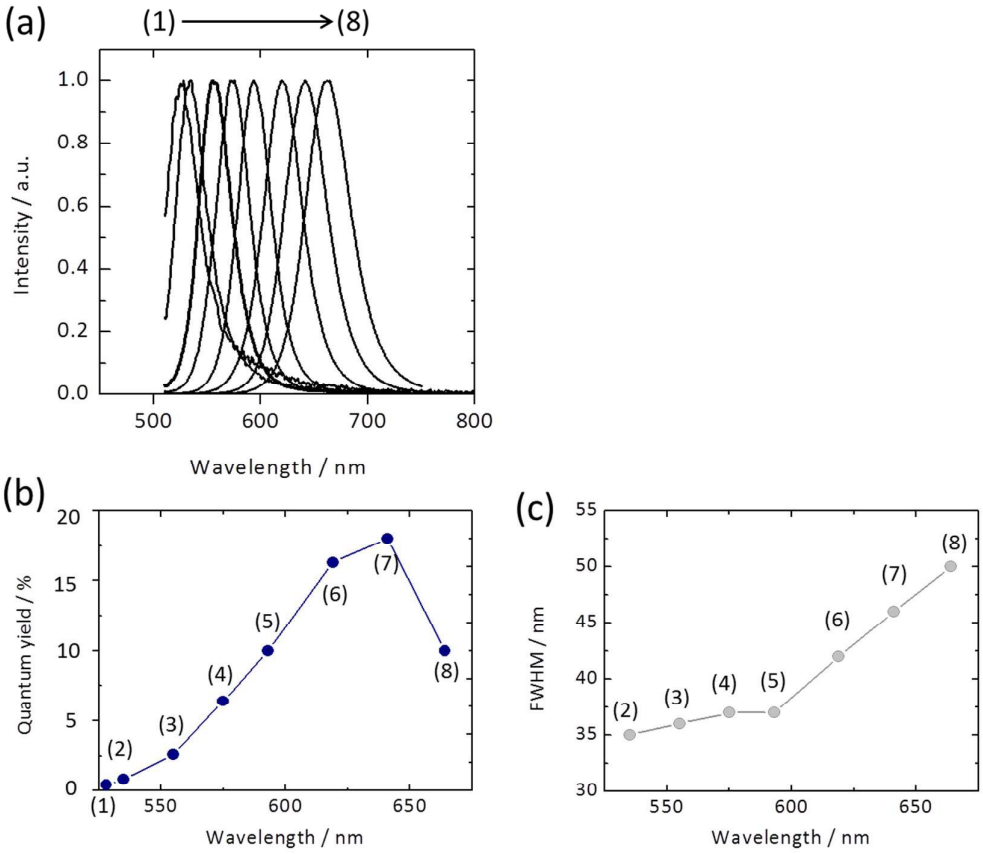

Figure 2. (a) Changes in emission spectra during CdTe growth, (b) evolution of quantum yield and (c) FWHM of the emission profile. Each plot represents the sample 1) 10 minutes, 2) 11 minutes, 3) 12 minutes, 4) 13 minutes, 5) 15 minutes, 6) 20 minutes, 7) 30 minutes and 8) 55 minutes after heating. Excitation wavelength = 500 nm.

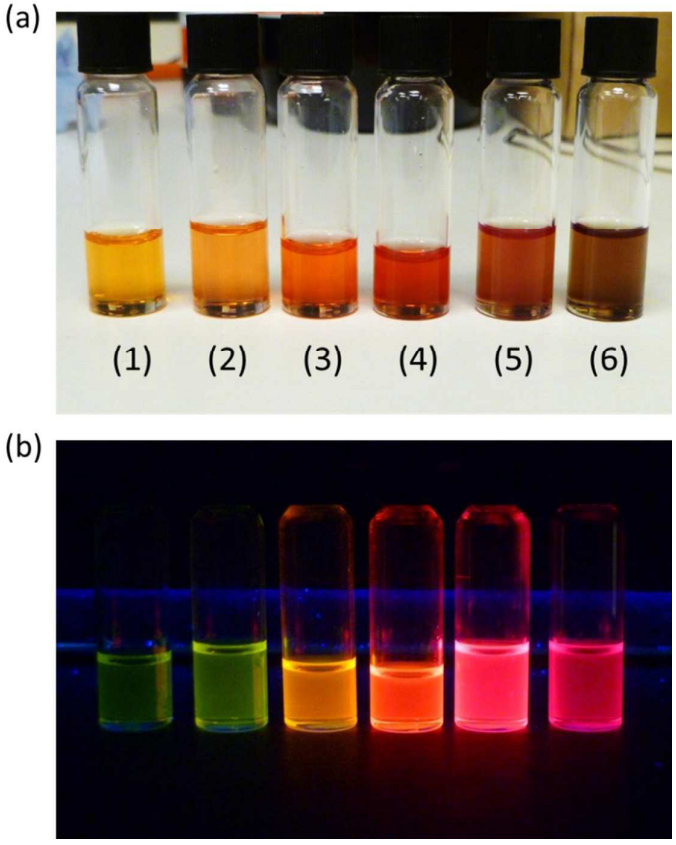

Figure 3. Images of CdTe QDs prepared from SSPs (a) under room light and (b) excitation at 365 nm. Each vial represents the sample prepared 1) 12 minutes, 2) 13 minutes, 3) 15 minutes, 4) 20 minutes, 5) 30 minutes and 6) 55 minutes after heating.

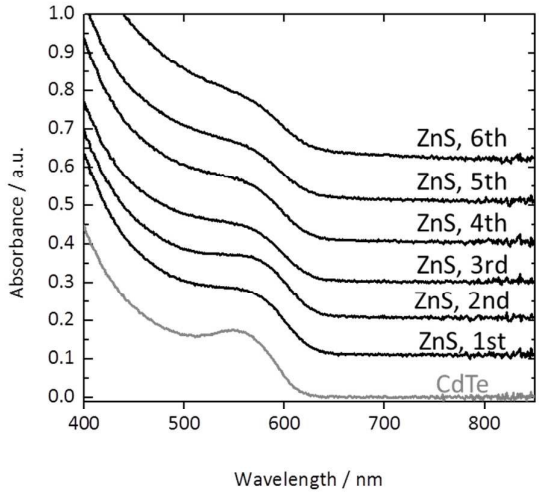

Figure 4. Absorption spectra during the ZnS shell deposition runs on a CdTe surface.

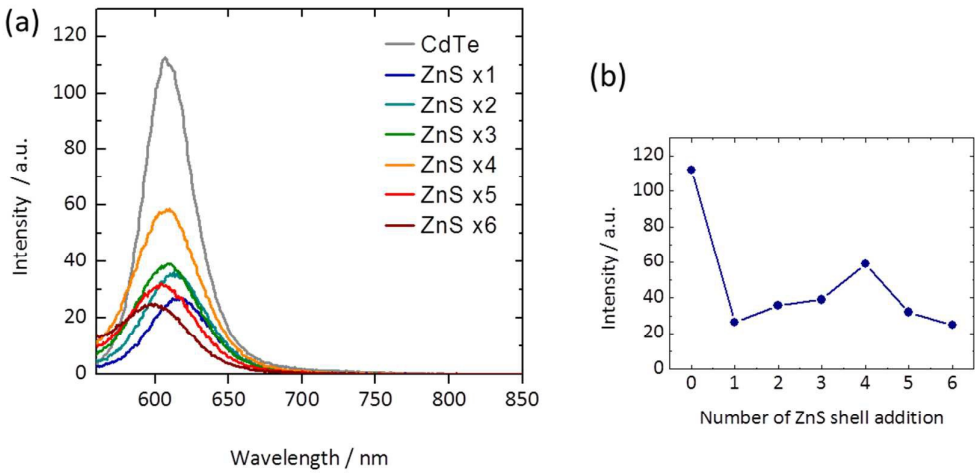

Figure 5 (a) Changes in emission spectra of CdTe QDs at each ZnS shell deposition (excitation wavelength = 500 nm). (b) Relationship between emission intensity and reaction stage.

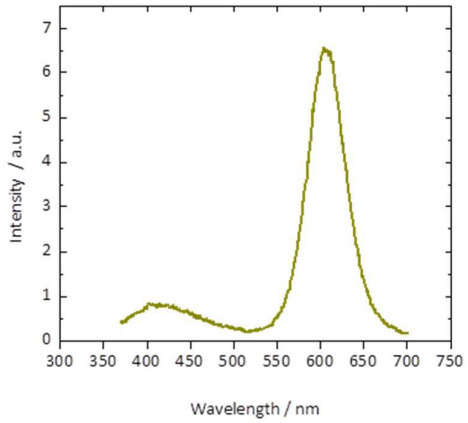

Figure 6. Emission spectrum of CdTe/ZnS QDs (6th ZnS shell addition) after purification (excitation wavelength 350 nm).

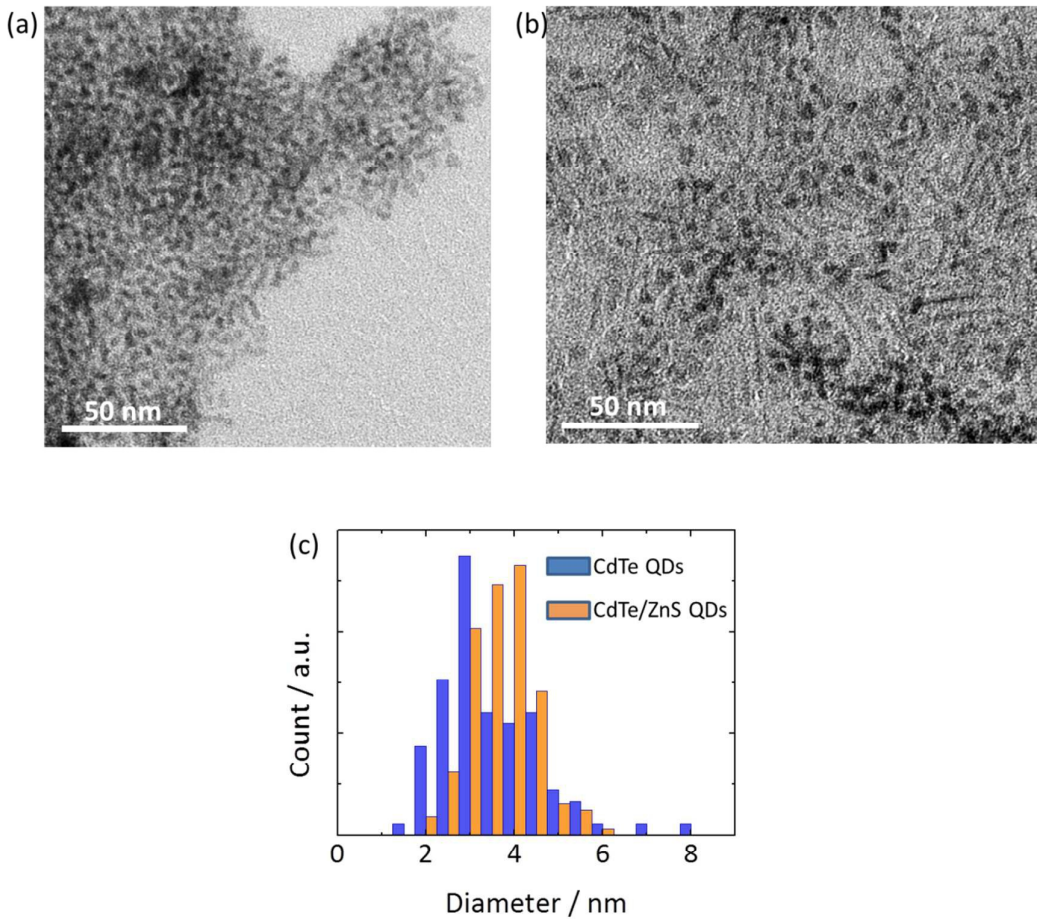

Figure 7. TEM images of (a) CdTe QDs prepared from SSPs and (b) CdTe/ZnS QDs after the 4th addition of $ZnDDTC_2$. (c) Size distribution of CdTe QDs and CdTe/ZnS QDs based on the TEM images.

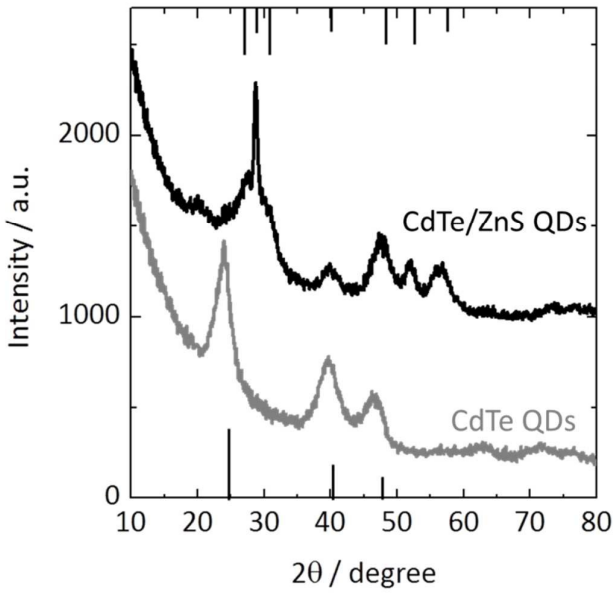

Figure 8. XRD patterns of CdTe QDs (grey curve) and CdTe/ZnS (4th shell deposition) QDs (black curve) prepared from SSPs. Millar indices for zinc blende CdTe (bottom) and wurtzite ZnS (top) are included as references.

References

1) M. Green, Semiconductor Quantum Dots: Organometallic and Inorganic Synthesis, RSC Nanoscience and Nanotechnology, 2014.

2) C. B. Murray, D. J. Norris, M. G. Bawendi, *J. Am. Chem. Soc.*, 1993**, 115**, 8706-8715.

3) S. L. Cumberland, K. M. Hanif, A. Javier, G. A. Khitrov, G. F. Strouse, S. M. Woessner, C. S. Yun, *Chem. Mater*., 2002**, 14**, 1576 -1584.

4) T. Trindade, P. O'Brien, X.-M. Zhang, M. Motevalli, *J. Mater. Chem*., 1997, **7**, 1011.

5) J. G. Brennan, T. Siegrist, P. J. Carroll, S. M. Stuczynski, P. Reynders, L. E. Brus, M. L. Steigerwald, *Chem. Mater*., 1990, **2**, 403.

6) M. A. Malik, M. Afzaal, P. O'Brien, *Chem. Rev*., 2010**, 110**, 4417-4446.

7) Y. A. Yang, H. M. Wu, K. R. Williams, Y. C. Cao, *Angew. Chem.-Int. Edit*., 2005**, 44**, 6712-6715.

8) S. S. Garje, J. S. Ritch, D. J. Eisler, M. Afzaal, P. O'Brien, T. Chivers, *J. Mater. Chem*., 2006**, 16**, 966-969.

9) M. L. Steigerwald, C. R. Sprinkle, *J. Am. Chem. Soc*., 1987**, 109**, 7200-7201.

10) K. Osakada, T. Yamamoto, *J. Chem. Soc. Chem. Commun*., 1987**,** 1117-1118.

11) J. G. Brennan, T.Siegrist, P. J. Carroll, S. M. Stuczynski, L. E. Brus, M. Steigerwald, *J. Am. Chem. Soc.*, 1989**, 111**, 4141-4143.

12) J. G. Brennan, T. Siegrist, P. J. Carroll, S. M. Stuczynski, P. Reynders, L. E. Brus, M. L. Steigerwald, *Chem. Mater*., 1990**, 2** , 403-409.

13) T. Trindade, P. O'Brien, *Adv. Mater*., 1996, **8**, 161-163.

14) T. Trindade, P. O'Brien, *J. Mater. Chem*., 1996, **6** , 343-347.

15) N. Revaprasadu, M. A. Malik, P. O'Brien, M. M. Zulu, G. Wakefield, *J. Mater. Chem*., 1998**, 8**, 1885-1888.

16) M. Lazell, P. O'Brien, *J. Chem. Soc., Chem. Commun.,* 1999**,** 2041-2042.

17) M. Lazell, S. J. Norager, P. O'Brien, N. Revaprasadu, *Mater. Sci. Eng. C-Biomimetic Supramol. Syst.,* 2001**, 16**, 129-133.

18) D. J. Crouch, P. O'Brien, M. A. Malik, P. J. Skabara, S. P. Wright, *J. Chem. Soc., Chem. Commun.,* 2003**,** 1454-1455.

19) Y. W. Jun, C. S. Choi, J. Cheon, *J. Chem. Soc*., Chem. Commun., 2001**,** 101-102.

20) S. M. Stuczynski, J. G. Brennan, M. L. Steigerwald, *Inorg. Chem.,* 1989**, 28**, 4431-4432.

21) M. Bochmann, G. Bwembya, K. J. Webb, M. A. Malik, J. R. Walsh, P. O'Brien, *Inorganic Syntheses*, 1997**, 31,** 19-24.

22) N. Ohira, Y. Aso, T. Otsubo, F. Ogura, *Chem. Lett.,* 1984**,** 13, 853-854.

23) M. Grabolle, M. Spieles, V. Lesnyak, N. Gaponik, A. Eychmuller, U. Resch-Genger, *Anal. Chem.,* 2009**, 81**, 6285-6294.

24) K. Rurack, M. Spieles, *Anal. Chem.,* 2011**, 83**, 1232-1242.

25) D. A. Chen, F. Zhao, H. Qi, M. Rutherford, X. G. Peng, *Chem. Mater*. 2010**, 22**, 1437-1444.

26) A. L. Rogach, T. Franzl, T. A. Klar, J. Feldmann, N. Gaponik, V. Lesnyak, A. Shavel, A. Eychmüller, Y. P. Rakovich, J. F. Donegan *J. Phys. Chem. C,* 2007**, 111**, 14628-14637.

27) N. Gaponik, D. V. Talapin, A. Rogach, K. Hoppe, E. V. Shevchenko, A. Kornowski, A. Eychmüller, H. Weller, *J. Phys. Chem. B*, 2002**, 106**, 7177-7185.

28) Y. Yin, A. P. Alivisatos, *Nature*, 2005**, 437**, 664-670.

29) W. W. Yu, Y. A, Wang, X. G. Peng, *Chem. Mater*., 2003**, 15**, 4300-4308.

30) D. V. Talapin, S. Haubold, A. L. Rogach, A. Kornowski, M. Haase, H. Weller, *J. Phys. Chem. B*, 2001**, 105**, 2260-2263.

31) N. Piven, A. S. Susha, M. Doeblinger, A. L. Rogach, *J. Phys. Chem. C*, 2008**, 112**, 15253-15259.

32) Y. Z. Tang, Y. Wang, S. Shanbhag, N. A. Kotov, *J. Am. Chem. Soc*., 2006**, 128**, 7036-7042.

33) W. W. Yu, L. H. Qu, W. Z. Guo, X. G. Peng, *Chem. Mater*., 2003**, 15**, 2854-2860.

34) A. M. Smith, A. M. Mohs, S. Nie, *Nat. Nanotechnol*., 2009**, 4**, 56-63.

35) J. R. Dethlefsen, A. Dossing, *Nano Lett*., 2011, **11**, 1964 – 1969.

36) W. Zhang, G. Chen, J. Wang, B.-C. Ye, X. Zhong, *Inorg. Chem*., 2009**, 48**, 9723-9731.

37) J. M. Tsay, M. Pflughoefft, L. A. Bentolila, S. Weiss, *J. Am. Chem. Soc*., 2004**, 126,** 1926-1927.

38) B. O. Dabbousi, J. Rodriguez-Viejo, F. V. Mikulec, J. R. Heine, H. Mattoussi, R. Ober, K. F. Jensen, M. G. Bawendi, *J. Phys. Chem. B*, 1997, **101**, 9463 – 9475.

39) M. T. Harrison, S. V. Kershaw, A. L. Rogach, A. Kornowski, A. Eychmüller, H. Weller, *Adv. Mater*., 2000, **12**, 123 – 125.

40) J. M. Pietryga, D. J. Werder, D. J. Williams, J. L. Casson, R. D. Schaller, V. I. Klimov, J. A. Hollingsworth, *J. Am. Chem. Soc*., 2008, **130**, 4879 – 4885.

41) D. C. Lee, I. Robel, J. M. Pietryga, V. I. Klimov, *J. Am. Chem. Soc*., 2010, **132**, 9960 – 9962.

42) F. V. Mikulec, PhD thesis, 1999, Massachusetts Institute of Technology.

43) J.-Y. Chang, S.-R. Wang, C.-H. Yang, *Nanotechnology*, 2007, **18**, 345602

44) M. Green, L. Sandiford, K. M. Anderson, Y. Ma., *ChemPlusChem.,* 2012, **77**, 192 - 195

45) M. Green, *J. Mater. Chem*., 2010**, 20**, 5797-5809.

46) M. Green, N. Allsop, G. Wakefield, P. J. Dobson, J. L. Hutchison, *J. Mater. Chem*., 2002**, 12**, 2671-2674.

47) A. J. Morris-Cohen, M. D. Donakowski, K. E. Knowles, E. A. Weiss, *J. Phys. Chem. C*, 2010**, 114**, 897-906.

48) D. V. Talapin, R. Koeppe, S. Götzinger, A. Kornowski, J. M. Lupton, A. L. Rogach, O. Benson, J. Feldmann, H. Weller, *Nano Lett*., 2003, **3**, 1677 - 1681.

49) X. H. Zhong, Y. Y. Feng, W. Knoll, M. Y. Han, *J. Am. Chem. Soc*., 2003**, 125**, 13559-13563.

50) S. Haubold, M. Haase, A. Kornowski, H. Weller, *ChemPhysChem*, 2001**, 2**, 331-334.

51) M. Protiere, P. Reiss, *Nanoscale Res. Lett*., 2006**, 1**, 62-67.

Graphical abstract

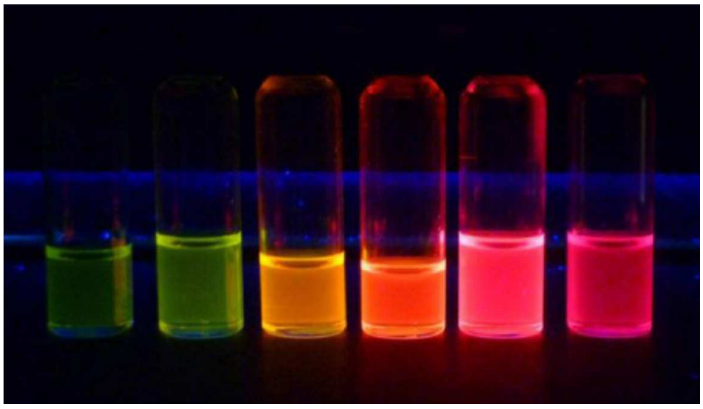

In this paper, we report the synthesis of CdTe/ZnS quantum dots using molecular single source precursors, and we explore the tuning of the optical properties.